Inorganic Chemistry

Article

pubs.acs.org/IC

Preparation and Magnetic Properties of Metal-Complexes from *N*-*t*-Butyl-*N*-oxidanyl-2-amino-(nitronyl nitroxide)

Takanori Furui,[†,§] Shuichi Suzuki,[†] Masatoshi Kozaki,[†] Daisuke Shiomi,[†] Kazunobu Sato,[†] Takeji Takui,[†] Keiji Okada,*[,†] Evgeny V. Tretyakov,[‡] Svyatoslav E. Tolstikov,[‡] Galina V. Romanenko,[‡] and Victor I. Ovcharenko*[,‡]

[†]Department of Chemistry, Graduate School of Science, Osaka City University, Sugimoto, Sumiyoshi-ku, Osaka 558-8585, Japan

[‡]International Tomography Center, Siberian Branch of the Russian Academy of Sciences, 3a ul. Institutskaya, 630090 Novosibirsk, Russian Federation

Supporting Information

ABSTRACT: Metal complexation reactions of *N*-*t*-butyl-*N*-oxidanyl-2-amino(nitronyl nitroxide) diradical (**1**) with M(hfac)$_2$ (M: Mn or Cu) were investigated. These reactions were found to be very sensitive to the type of metal ion employed. Complex [Mn(hfac)$_2$·**1**], consisting of Mn(hfac)$_2$ and diradical **1**, was readily prepared by mixing the components. However, the reaction of Cu(hfac)$_2$ with **1** or *N*-*t*-butyl-*N*-oxidanyl-2-amino(iminonitroxide) diradical (**2**) involved the reduction of the diradical to the *N*-*t*-butyl-*N*-oxidanide-2-amino(iminonitroxide) radical anion (**3**) and finally produced the polymer-chain complex [Cu$_2$(hfac)$_2$·**3**$_2$·Cu(hfac)$_2$]$_n$. The structures of these complexes were elucidated by X-ray analysis, and their magnetic properties were investigated in detail. The temperature dependence of χ_pT (χ_p: magnetic susceptibility) for [Mn(hfac)$_2$·**1**] exhibited a strong antiferromagnetic interaction ($H = -2JS_1 \cdot S_2$, $J/k_B = -217$ K) between the Mn(II) spin ($S = 5/2$) and the diradical **1** spin ($S = 1$). However, the χ_pT-T plots for [Cu$_2$(hfac)$_2$·**3**$_2$·Cu(hfac)$_2$]$_n$ indicated the presence of several magnetic interactions: a large ferromagnetic interaction ($J/k_B = 510$ K) between iminonitroxide **3** and the imino-coordinating Cu(II) atom, a moderately large ferromagnetic interaction ($J/k_B = 58$ K) between the iminonitroxide and (iminonitroxide oxygen)-coordinating Cu(hfac)$_2$, and a weak antiferromagnetic interaction ($J/k_B = -1.4$ K) between the two Cu(hfac)-**3** moieties within a Cu$_2$O$_2$ square.

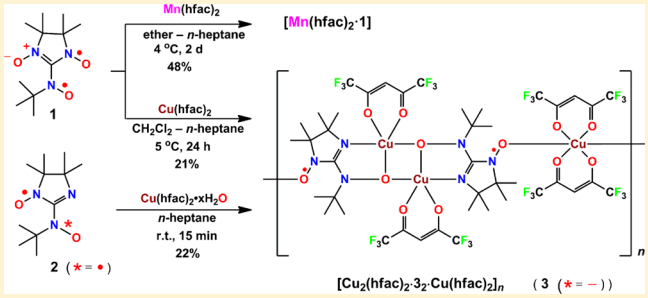

1. INTRODUCTION

Stable, organic, open-shell molecules have garnered great attraction because of their wide diversity in molecular design and processability,[1,2] which facilitates their application in molecule-based magnets,[1,3] electrical conductors,[4,5] contrast agents for magnetic resonance tomography,[6] radical-based rechargeable batteries,[7] spintronic devices,[4,5,7,8] and molecular spin-based quantum computers.[9] In addition to these developments, the synthesis of high-spin molecules are also attracting increasing attention.[1−3] Of these, trimethylenemethane (TMM) is the simplest species that shows a large and positive exchange interaction,[10] although it undergoes a facile ring-closure reaction at temperatures above 123 K.[11] Thus far, several stable diradicals and polyradicals have been designed and synthesized using *m*-phenylene- and alkylidene-bridged nitronyl nitroxides (NN) and iminonitroxides (IN). However, only a few stable diradicals have been reported to exhibit large exchange interactions, $J/k_B > +300$ K, $H = -2JS_1 \cdot S_2$.[12]

Recently, highly compact TMM-analogues, **1** and **2** (see Scheme 1 and Scheme 2), have been synthesized using NN, IN, and *t*-butyl nitroxide as spin sources by two groups (present authors in Japan and Russia).[13] During an international workshop between the two countries (the sixth Russian-Japanese workshop) and the 13th International Conference on Molecule-based Magnets (ICMM 2012), we have cooperatively investigated transition-metal complexes derived from **1** and **2**. In particular, we found that the formation of metal complexes using these ligative diradicals[14] is sensitive to the type of metal employed. Although the [Mn(hfac)$_2$·**1**] complex was readily prepared by mixing Mn(hfac)$_2$ and diradical **1**, the corresponding Cu(hfac)$_2$ complex could not be obtained from either **1** or

Scheme 1. Complexation of Mn(hfac)$_2$ with Diradical 1

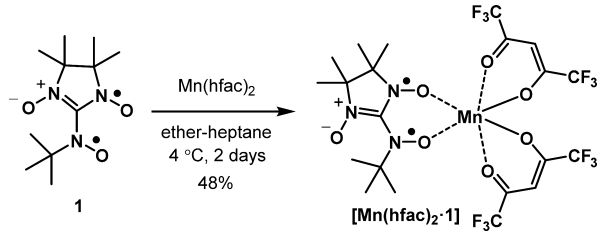

Received: August 18, 2013
Published: December 23, 2013

   dx.doi.org/10.1021/ic4020898 | *Inorg. Chem.* 2014, 53, 802−809

Scheme 2. Complexation of $Cu(hfac)_2$ with Diradical 1 or 2

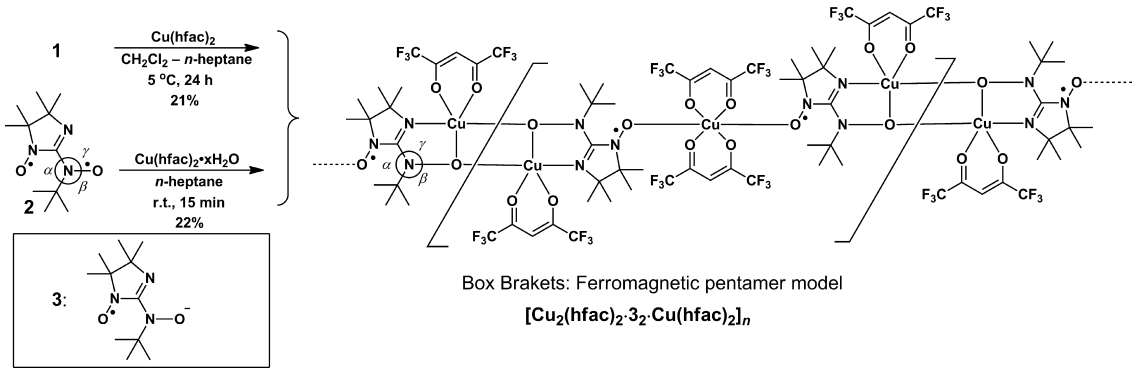

2; moreover, redox reactions involving the decomposition of **1** and **2** to yield the paramagnetic radical anion **3** occurred to give $[Cu_2(hfac)_2{\cdot}\mathbf{3}_2{\cdot}Cu(hfac)_2]_n$ from both **1** and **2** (see Scheme 2). Herein, we report the preparations, molecular and packing structures, and magnetic properties of $[Mn(hfac)_2{\cdot}\mathbf{1}]$ and $[Cu_2(hfac)_2{\cdot}\mathbf{3}_2{\cdot}Cu(hfac)_2]_n$.

2. EXPERIMENTAL SECTION

General Procedures. The chemicals were of commercial grade and were used without further purification. Melting points were measured using a Yanako MP-J3 apparatus, and they were not corrected. The infrared spectra were measured using a Shimadzu FTIR-8700. The X-ray data were collected by a Rigaku CCD and Smart Apex II (Bruker AXS) area detectors with graphite-monochromated Mo−Kα radiation. The structures were resolved by a direct method (SIR92 or SHELX97) and expanded using a Fourier technique. All the calculations were performed using the Crystal Structure crystallographic software package. The magnetic susceptibility measurements were performed using a Quantum Design SQUID magnetometer, MPMS-*XL*.

Preparation of $[Mn(hfac)_2{\cdot}\mathbf{1}]$. A suspension of bis(hexafluoroacetylacetonato)manganese(II) ($Mn(hfac)_2{\cdot}3H_2O$, 120 mg, 0.256 mmol) in *n*-heptane (30 mL) was refluxed for 1 h. Then, the solvent (~20 mL) was distilled off to remove water involved in $Mn(hfac)_2{\cdot}3H_2O$ as an azeotrope. To the dried yellow *n*-heptane solution (10 mL) of $Mn(hfac)_2$, an ether solution (1 mL) of **1** (61.8 mg, 0.255 mmol) was added at room temperature. Crystals were produced by slow evaporation of ether at 4 °C for 2 days in a glovebox; these were then collected by filtration and washed with cold *n*-heptane, to yield $[Mn(hfac)_2{\cdot}\mathbf{1}]$ as black green blocks (91.5 mg, 50%). $[Mn(hfac)_2{\cdot}\mathbf{1}]$: mp 108 °C (decomp.); IR (KBr, cm^{-1}): 3005, 2947, 1651, 1556, 1529, 1483, 1377, 1256, 1215, 1148, 1099, 799, 665; anal. calcd. for $C_{21}H_{23}F_{12}MnN_3O_7$ (MW 712.34): C, 35.41; H, 3.25; N, 5.90; found: C, 35.41; H, 3.28; N, 5.94; ESR (powder): g = 2.043; crystallographic data for $[Mn(hfac)_2{\cdot}\mathbf{1}]$: monoclinic, space group: $C2/c$ (#15), a = 25.1960(13) Å, b = 8.5524(4) Å, c = 27.5246(16) Å, $\alpha = \gamma$ = 90.0°, β = 90.202(3)°, V = 5931.1(5) Å^3, Z = 8; D_{calcd} = 1.596 g cm^{-3}, T = 150(2) K; R = 0.0648, R_w = 0.1486, GOF = 1.091.

Preparation of $[Cu_2(hfac)_2{\cdot}\mathbf{3}_2{\cdot}Cu(hfac)_2]_n$. Complex $[Cu_2(hfac)_2{\cdot}\mathbf{3}_2{\cdot}Cu(hfac)_2]_n$ was prepared by the following two routes (a) and (b).

(a). From the Reaction of $Cu(hfac)_2$ with Diradical ***1****.* The mixture of bis(hexafluoroacetylacetonato)copper(II) $Cu(hfac)_2$ (76 mg, 0.16 mmol, sublimed (150−160 °C/0.5 mmHg) before use) and **1** (40 mg, 0.16 mmol) was dissolved in dichloromethane (2 mL), and *n*-heptane (1 mL) was added. Slow evaporation of the solvent at 4 °C for 12 h produced an unidentified oily material looking like a black film on the bottom of the glass surface. This tar-like material was removed by decantation, and the solution was stored at 4 °C for 12 h. The produced black crystals were filtered off and washed with *n*-heptane to yield $[Cu_2(hfac)_2{\cdot}\mathbf{3}_2{\cdot}Cu(hfac)_2]_n$ (25 mg, 21%).

(b). From the Reaction of $Cu(hfac)_2$ with Diradical ***2****.* $Cu(hfac)_2$ (148.9 mg, 0.312 mmol) and diradical **2** (84.9 mg, 0.373 mmol) were dissolved in *n*-heptane (13 mL). The mixture was stirred for 15 min at room temperature and then filtered through a syringe filter (DISMIC-25, pore size 0.50 μm) to remove any insoluble materials. Slow evaporation of *n*-heptane at 4 °C produced crystals, which were collected by filtration and washed with dichloromethane to yield $[Cu_2(hfac)_2{\cdot}\mathbf{3}_2{\cdot}Cu(hfac)_2]_n$ as black blocks (33.9 mg, 22%). $[Cu_2(hfac)_2{\cdot}\mathbf{3}_2{\cdot}Cu(hfac)_2]_n$: m.p.: 174 °C (decomp.); IR (KBr, cm^{-1}): 2986, 2943, 1647, 1556, 1475, 1332, 1259, 1223, 1207, 1148, 1111, 804, 795, 682, 675; anal. calcd. for $C_{42}H_{46}Cu_3F_{24}N_6O_{12}$ (MW 1473.45): C, 34.24; H, 3.15; N, 5.70; found: C, 34.41; H, 3.26; N, 5.90; crystallographic data: triclinic, space group: $P\bar{1}$ (#2), a = 10.5121(8) Å, b = 11.1887(9) Å, c = 13.1320(11) Å, α = 76.799(6)°, γ = 88.361(6)°, β = 73.751(5)°, V = 1442.6(2) Å^3; Z = 1; D_{calcd} = 1.696 g cm^{-3}; T = 240(2) K; R = 0.0429, R_w = 0.0708, GOF = 0.786.

3. RESULTS AND DISCUSSION

Preparation of Metal Complexes from 1 and 2. Diradical **1** underwent a complexation reaction with $Mn(hfac)_2$ in an *n*-heptane-ether mixture to form $[Mn(hfac)_2{\cdot}\mathbf{1}]$, which was obtained as good crystals suitable for X-ray analysis (Scheme 1).

Similar treatment of an *n*-heptane-dichloromethane solution of $Cu(hfac)_2$ with diradical **1** produced good black crystals (21% yield) of a polymer-chain complex $[Cu_2(hfac)_2{\cdot}\mathbf{3}_2{\cdot}Cu(hfac)_2]_n$, in which radical anion **3** is formed by the decomposition of diradical **1** (Scheme 2). The decomposition of diradical **1** occurred in the presence of $Cu(hfac)_2$ even under argon ($[O_2]$~1 ppm in a glovebox) in various solvents such as toluene, ether, and acetonitrile. The use of a different Cu(II) source ($Cu(ClO_4)_2$ or $Cu(O_2CCF_3)_2$) in acetonitrile or acetonitrile-mixed solvents also induced the decomposition. The decomposition also occurred even under dried conditions (solvents and Cu(II) sources), although participation of a small amount of water in this decomposition could not be ruled out. The decomposition was not observed in the absence of Cu(II) ions under the same conditions.

The first step of the decomposition could be the deoxygenation of diradical **1** induced by the Cu(II)-oxidant with the formation of diradical **2** and Cu(I) species. Although the mechanistic details of the deoxygenation pathway are uncertain, the conversion of diradical **1** to iminonitroxide **2** was confirmed by monitoring the reaction by TLC. The oxidative deoxygenation path can be supported by the following observations in the literatures: Nitronyl nitroxides can be converted into iminonitroxides in the presence of an electron-deficient and oxygen-accepting TCNQ and/or $TCNQF_4$,[15] in the reaction with chlorine gas followed by treatment with

dx.doi.org/10.1021/ic4020898 | *Inorg. Chem.* 2014, 53, 802−809

ethanol,[16] and also in the reaction with MnO_2 in nitromethane.[17] In the next step, diradical **2** would be reduced under the complexation conditions to give the paramagnetic anion **3**. The occurrence of this step is supported by the formation of the same complex $[Cu_2(hfac)_2{\cdot}\mathbf{3}_2{\cdot}Cu(hfac)_2]_n$ in the reaction of $Cu(hfac)_2$ with diradical **2** (Scheme 2).

Structures of Metal Complex, $[Mn(hfac)_2{\cdot}\mathbf{1}]$ and $[Cu_2(hfac)_2{\cdot}\mathbf{3}_2{\cdot}Cu(hfac)_2]_n$. Figure 1 shows the molecular

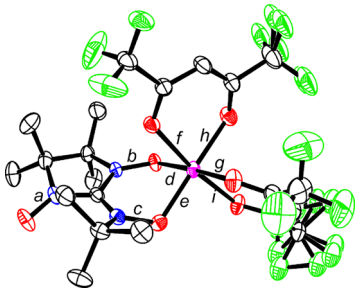

Figure 1. Molecular structure of $[Mn(hfac)_2{\cdot}\mathbf{1}]$ drawn at a 50% ellipsoid level, in which a disorder is observed in the hfac moieties and all hydrogen atoms are omitted for clarity. Typical bond lengths: *a*: 1.267(3) (1.273(3)), *b*: 1.311(3) (1.276(2)), *c*: 1.335(2) (1.282(2)), *d*: 2.019(2), *e*: 1.988(2), *f*: 2.171(2), *g*: 2.060(2), *h*: 2.064(2), *i*: 2.135(2) Å; the parentheses values are bond lengths of diradical **1**.

structure of $[Mn(hfac)_2{\cdot}\mathbf{1}]$ obtained from the X-ray analysis; the crystallographic data are summarized in Table 1. The $[Mn(hfac)_2{\cdot}\mathbf{1}]$ complex showed a disorder in the hfac moieties. The N−O bond lengths in the radical moiety slightly increased by the coordination to the Mn(II) atom (bonds *b* and *c* in Figure 1) compared with the N−O bond lengths of free diradical **1**[13] (parentheses values in bond *b* and *c* in Figure 1). The torsion angle between the ONCNO plane in the nitronyl nitroxide and *t*-Bu nitroxide plane (73° in free **1**) decreased to 29° because of the coordination to the Mn(II) atom. The Mn−O_{hfac} bonds (*f*: 2.171(2), *g*: 2.060(2), *h*: 2.064(2), *i*: 2.135(2) Å, Figure 1) in the hfac moieties were slightly longer than the Mn−O_{NO} bonds (*d*: 2.019(2), *e*: 1.988(2) Å), suggesting a stronger bonding character of the Mn−O_{NO} bonds.

For the intermolecular contacts between magnetically important elements, we found two identical intermolecular contacts (O---C: 3.32 Å) between the NO oxygen atom and the methyl carbon atom in the *t*-Bu group of the adjacent $[Mn(hfac)_2{\cdot}\mathbf{1}]$ group (Figure 4, red dotted lines).

The linear chain structure $[Cu_2(hfac)_2{\cdot}\mathbf{3}_2{\cdot}Cu(hfac)_2]_n$ determined by the X-ray analysis is shown in Figure 2. The crystallographic data are collected in Table 1. The NO group in bond *a* (1.265(2) Å), which weakly coordinates to the Cu(II) atom (*h*: 2.702(3) Å), had a typical bond length for nitroxides (1.275(2) Å in **2**).[13] However, the N−O bond *c* (1.428(3) Å) in the *t*-BuNO moiety was considerably longer (compared with 1.281(2) Å in **2**),[13] indicating the presence of an oxygen anion in the *t*-BuNO moiety of the Cu complex. Furthermore, the summation of the bond angles around the nitrogen atom (α, β, and γ denoted in Scheme 2) of the *t*-BuNO moiety in the Cu complex was 336.4° (α: 120.4(2)°, β: 108.8(2)°, γ: 107.2(2)°) in contrast to free diradical **2** (total: 359.7°, α: 121.8(2)°, β: 120.3(2)°, γ: 117.6(2)° in Scheme 2), indicating that the nitrogen atom in the *t*-BuNO moiety of the Cu complex has a $sp^{2+\delta}$ hybridization; being compatible with the anionic oxygen atom of the *t*-BuNO moiety in the Cu complex.

Table 1. Crystallographic Data of $[Mn(hfac)_2{\cdot}\mathbf{1}]$[a] and $[Cu_2(hfac)_2{\cdot}\mathbf{3}_2{\cdot}Cu(hfac)_2]_n$[b]

	$[Mn(hfac)_2{\cdot}\mathbf{1}]$[a]	$[Cu_2(hfac)_2{\cdot}\mathbf{3}_2{\cdot}Cu(hfac)_2]_n$[b]
formula	$C_{21}H_{23}F_{12}MnN_3O_7$	$C_{42}H_{46}Cu_3F_{24}N_6O_{12}$
formula weight	712.35	1473.46
crystal color, morphology	black, prism	black, plate
crystal size/mm	0.38 × 0.32 × 0.32	0.20 × 0.08 × 0.02
crystal system	monoclinic	triclinic
space group	*C*2/*c* (#15)	$P\bar{1}$ (#2)
a/Å	25.1960(13)	10.5121(8)
b/Å	8.5524(4)	11.1887(9)
c/Å	27.5246(16)	13.1320(11)
α/degree		76.799(6)
β/degree	90.202(3)	88.361(6)
γ/degree		73.751(5)
V/Å^3	5931.1(5)	1442.6(2)
Z value	8	1
T/K	150(2)	240(2)
D_{calc}/g cm^3	1.596	1.696
F(000)	2872	739
μ/ cm^{-1}	5.64 (Mo−Kα)	12.34 (Mo−Kα)
no. of reflections measured	21901	23277
no. of unique reflections	6588	6728
no. of observed reflections	6588 ($I > 2.00\sigma(I)$)	3258 ($I > 2.00\sigma(I)$)
no. of variables	415	502
reflection/parameter ratio	15.87	6.49
R1 [$I > 2.00\sigma(I)$][c]	0.0648	0.0429
R_w[d]	0.1486[e]	0.0708[f]
goodness-of-fit	1.091	0.786

[a]CCDC#: CCDC 956311. [b]CCDC#: CCDC 956312. [c]$R1 = \sum||F_o| - |F_c||/\sum|F_o|$. [d]$R_w = [\sum(w(F_o^2 - F_c^2)^2)/\sum w(F_o^2)^2]^{1/2}$. [e]$w = 1/[\sigma^2(F_o^2) + (0.0594P)^2 + 25.1447P]$ where $P = (F_o^2 + 2F_c^2)/3$. [f]$w = 1/[\sigma_2(F_o^2) + (0.0310P)^2]$ where $P = (F_o^2 + 2F_c^2)/3$.

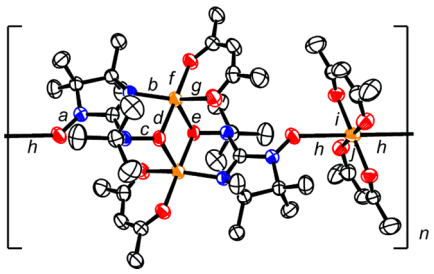

Figure 2. Molecular structure of the repeating unit $[Cu_2(hfac)_2{\cdot}\mathbf{3}_2{\cdot}Cu(hfac)_2]_n$ drawn at a 50% ellipsoid level, in which all hydrogen and fluorine atoms are omitted for clarity. Typical bond lengths: *a*: 1.265(2), *b*: 1.960(2), *c*: 1.428(3), *d*: 1.921(2), *e*: 2.199(2), *f*: 1.951(2), *g*: 1.997(2), *h*: 2.703(2), *i*: 1.924(2), *j*: 1.913 (2) Å.

A square composed of two Cu atoms and two anionic oxygen atoms of *t*-BuNOs was observed in the Cu complex, $[Cu_2(hfac)_2{\cdot}\mathbf{3}_2{\cdot}Cu(hfac)_2]_n$. The bond angle of Cu−O−Cu was 97.38(8)° with a Cu---Cu distance of 3.10 Å. The Cu atoms within the square occupied the penta-coordinated square pyramidal geometry with one Cu−$N_{C=N}$ bond (*b*: 1.960(2) Å), two Cu−O_{hfac} bonds (*g*: 1.997(2) Å and *f*: 1.951(2) Å), and two Cu−$O_{t\text{-}BuNO}$ bonds (*d*: 1.921(2) Å and *e*: 2.199(2) Å (axial)) within the Cu−O−Cu-O square. The structures of

dx.doi.org/10.1021/ic4020898 | Inorg. Chem. 2014, 53, 802−809

Cu(II) dimers involving a Cu_2O_2 square moiety have frequently been observed.[18] The relationship between the exchange interaction and the Cu−O−Cu angle in hydroxo-briged Cu(II) dimers has also been reported.[19] Based on these studies, the Cu atoms in the Cu_2O_2 square in $[Cu_2(hfac)_2{\cdot}\mathbf{3}_2{\cdot}Cu(hfac)_2]_n$ can be safely assigned as Cu(II) species.

Magnetic Properties of [Mn(hfac)$_2$·1]. Figure 3 shows the temperature dependence of χ_pT (χ_p: molar paramagnetic susceptibility) of $[Mn(hfac)_2{\cdot}\mathbf{1}]$. The χ_pT value at room temperature was approximately 2.05 emu·K·mol^{-1}, which gradually decreased to reach a plateau (1.94 emu·K·mol^{-1}) with decreasing temperature (300 → 150 K). This behavior can be explained using the antiferromagnetic spin pair model:

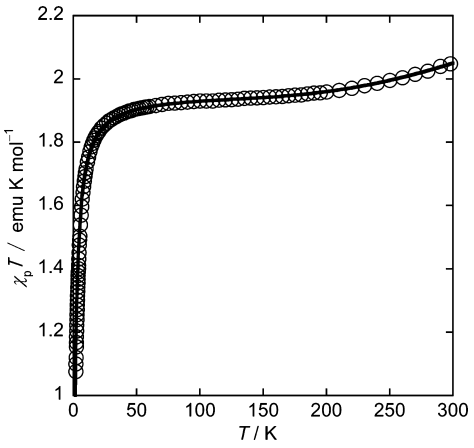

Figure 3. χ_pT−T plot of $[Mn(hfac)_2{\cdot}\mathbf{1}]$; the black circle indicates the observed value of χ_pT measured under an external magnetic field of 1,000 G and the solid line indicates a simulation curve with parameters of g = 2.043, J/k_B = −217 K, and θ = −1.40 K in eq 2.

$$H = -2J\mathbf{S}(\mathrm{Mn})\cdot\mathbf{S}(\mathbf{1}) \quad (1)$$

The parameter J denotes the exchange interaction between Mn(II) (S(Mn) = 5/2) and **1** (S(**1**) = 1) in the spin pair. The temperature-dependence of χ_pT was reproduced by assuming thermal equilibrium for each spin state

$$\chi_pT = \frac{N_A g^2 \mu_B{}^2 T}{3k_B(T-\theta)} \cdot \frac{\sum_i s_i(s_i+1)(2s_i+1)\exp(-\varepsilon_i/k_BT)}{\sum_i (2s_i+1)\exp(-\varepsilon_i/k_BT)} \quad (2)$$

with a total spin of $\mathbf{s}_i = S(\mathrm{Mn}) + S(\mathbf{1})$ (s_1 =7/2, s_2 =5/2, s_3 =3/2, ε_1= −12J, ε_2= −5J, and ε_3= 0) under the mean-field approximation of interpair interaction θ. The solid line in Figure 3 represents a simulation line with parameters g = 2.043, J/k_B = −217 K, and θ = −1.40 K in eq 2.

These magnetic interactions should have structural origins. The large J/k_B = −217 K is obviously attributed to the intramolecular antiferromagnetic interaction between Mn(II) and **1**. To get an insight into the small magnetic interaction of θ = −1.40 K, we calculated magnetic interactions on intermolecular spin pairs. We searched for short intermolecular contacts between magnetically important elements (see Structures of Metal Complex section) and found two equivalent short intermolecular contacts between the NO oxygen atom in the $[Mn(hfac)_2{\cdot}\mathbf{1}]$ complex and the methyl carbon atom of the *t*-Bu group in the adjacent $[Mn(hfac)_2{\cdot}\mathbf{1}]$ complex (3.32 Å, red dotted lines within $[Mn(hfac)_2{\cdot}\mathbf{1}]_2$-A, B, and C in Figure 4). The lengths of these intermolecular O---C contacts are close to the summation (3.3 Å) of their respective van der Waals radii. With this geometry, two spin states, high-spin (S = 3, $[Mn(hfac)_2{\cdot}\mathbf{1}]_2$-B in Figure 4) and low-spin (S = 0, $[Mn(hfac)_2{\cdot}\mathbf{1}]_2$-C), are possible. The energies of these states for the geometry determined by X-ray analysis were estimated using the Gaussian 09 program package with a ub3lyp/6-31G* level theory.[20] The energy difference (ΔE = −5.95 K, the minus sign means higher stability of the low-spin state) is calculated from the high- ($E_{Stotal=3}$ = −7707.08303137 au, $\langle S^2\rangle$ = 14.7925) and low-spin ($E_{Stotal=0}$ = −7707.08305024 au, $\langle S^2\rangle$ = 5.7925) states. The total energy calculated using a UHF-SCF procedure involves spin-contamination contributed from higher spin states. To estimate the exchange interaction (J/k_B between two spins $\mathbf{S}_a$ and $\mathbf{S}_b$, $H = -2J\mathbf{S}_a\cdot\mathbf{S}_b$), we used a spin projection method (eq 3) proposed by Yamaguchi and co-workers.[21]

$$J = \frac{{}^{LS}E - {}^{HS}E}{\langle {}^{HS}S^2\rangle - \langle {}^{LS}S^2\rangle} \quad (3)$$

where ${}^{LS}E$ and ${}^{HS}E$ are the total energies, and $\langle {}^{LS}S^2\rangle$ and $\langle {}^{HS}S^2\rangle$ are the $\langle S^2\rangle$ values for the low-spin and high-spin states, respectively. Thus, the corrected magnetic interaction was estimated to be J/k_B = −0.66 K in the $[Mn(hfac)_2{\cdot}\mathbf{1}]_2$ case. The estimated value is approximately equivalent to the experimentally determined value of θ = −1.40 K.

The calculated total energies (E/au), $\langle S^2\rangle$ values, energy differences ($\Delta E_{LS\text{-}HS}$/K) between low- and high-spin states, and

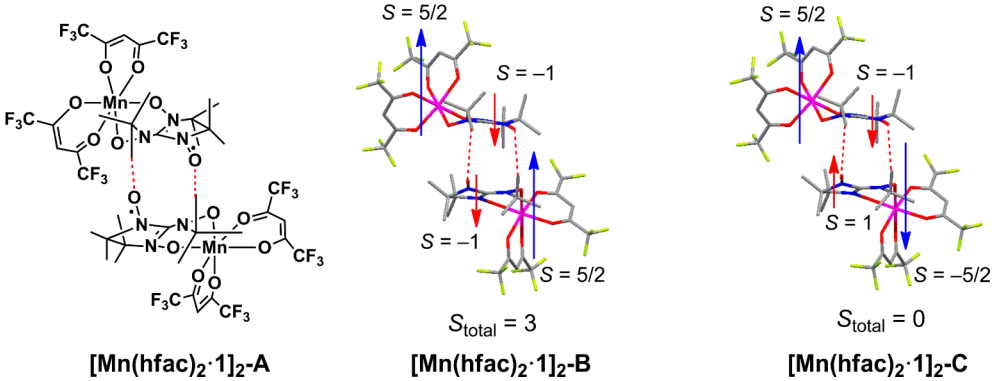

Figure 4. Intermolecular contacts (red dashed line: 3.318 Å) of $[Mn(hfac)_2{\cdot}\mathbf{1}]$ (**A**: chemical formula, **B**: high-spin structure (S_{total} = 3), and **C**: low spin structure (S_{total} = 0).

dx.doi.org/10.1021/ic4020898 | *Inorg. Chem.* 2014, 53, 802−809

Table 2. Calculated Total Energies for Low- And High-Spin States of Model Compounds Shown in Figures 4 and 6−8

compounds and spin states	E/au	$\langle S^2 \rangle$	energy difference ($\Delta E_{LS\text{-}HS}$)/K	exchange interaction (J)/K
$[Mn(hfac)_2\cdot\mathbf{1}]_2$-**B** ($S_{total}$ = 3) in Figure 4	−7707.08303137	14.7925	−5.95	−0.66
$[Mn(hfac)_2\cdot\mathbf{1}]_2$-**C** ($S_{total}$ = 0) in Figure 4	−7707.08305024	5.7925		
[Cu(hfac)·**3**·ONH^{t}Bu]-**B** (S_{total} = 1) in Figure 6	−3615.37602285	2.0419	+520	+510
[Cu(hfac)·**3**·ONH^{t}Bu]-**C** (S_{total} = 0) in Figure 6	−3615.37437367	1.0236		
$[Cu(hfac)\cdot\mathbf{3}]_2$-**B** ($S_{total}$ = 2) in Figure 7	−6654.23070691	6.0212	−29.3	−7.33
$[Cu(hfac)\cdot\mathbf{3}]_2$-**C** ($S_{total}$ = 0) in Figure 7	−6654.23079997	2.0173		
[**3**·$Cu(hfac)_2$·**3**]-**B** (S_{total} = 3/2) in Figure 8	−5013.82350479	4.0151	+114	+57.6
[**3**·$Cu(hfac)_2$·**3**]-**C** (S_{total} = 1/2) in Figure 8	−5013.82314218	2.0293		

exchange interactions (J/k_B/K, $H = -2J\mathbf{S}_a\cdot\mathbf{S}_b$) for the Mn- and Cu-complexes are summarized in Table 2.

Magnetic Properties of $[Cu_2(hfac)_2\cdot\mathbf{3}_2\cdot Cu(hfac)_2]_n$. The temperature dependence of the χ_pT values of $[Cu_2(hfac)_2\cdot\mathbf{3}_2\cdot Cu(hfac)_2]_n$ is shown in Figure 5. The χ_pT value at room temperature was 2.448 emu·K·mol^{-1}. When the temperature was lowered, the χ_pT value gradually increased to a broad maximum value (2.515 emu·K·mol^{-1}) at approximately 150 K and slowly decreased to 2.343 emu·K·mol^{-1} at approximately 50 K (Supporting Information, Figure S1). Below 50 K, the χ_pT value steeply decreased (0.188 emu·K·mol^{-1} at 2.0 K). The χ_p-T plot (Figure 5 inset) had a maximum at approximately 10 K.

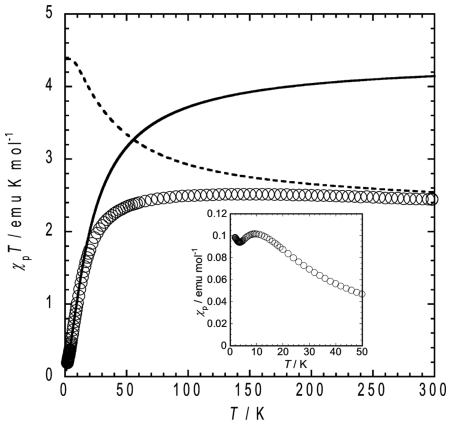

Figure 5. χ_pT-T plot of $[Cu_2(hfac)_2\cdot\mathbf{3}_2\cdot Cu(hfac)_2]_n$; the black circles indicate the observed value of χ_pT measured under an external magnetic field of 1,000 G. Inset: the χ_p-T plot showing a maximum value around 10 K. The dashed line: the simulation line based on the ferromagnetic pentamer model (J_1/k_B = +510 K, J_2/k_B = +58 K) in Scheme 3. The solid line: the simulation line based on the equally spaced antiferromagnetic Fisher chain model (J/k_B = −1.4 K).

These results indicate that there are at least two magnetic interactions; one is a considerably large ferromagnetic interaction of the order of several hundred kelvins, and the other is a weak antiferromagnetic interaction of the order of several kelvins or tens of kelvins as suggested from the maximum in the χ_p-T plot (Figure 5 inset).

The linear chain complex $[Cu_2(hfac)_2\cdot\mathbf{3}_2\cdot Cu(hfac)_2]_n$ consists of several magnetic components (Figure 2). Consequently, direct simulation of the experimental χ_pT-T plot (Figure 5) was difficult. Fortunately, each of the magnetic interactions could be theoretically extracted from the X-ray structure of $[Cu_2(hfac)_2\cdot\mathbf{3}_2\cdot Cu(hfac)_2]_n$. First, we focused on the structure of the •O−N−C═N−Cu(II) moiety (formulated by [Cu(hfac)·**3**·ONH^{t}Bu]-A, B, C in Figure 6). A similar pentacoordinated Cu(II) complex with iminonitroxide has been reported to have a large ferromagnetic interaction by Rey and co-workers.[22] We calculated the energy difference (ΔE = +520 K in Table 2) between the high-spin (**B**, $E_{Stotal=1}$ = −3615.37602285 au, $\langle S^2 \rangle$ = 2.0419) and low-spin (**C**, $E_{Stotal=0}$ = −3615.37437367 au, $\langle S^2 \rangle$ = 1.0236) states. The magnetic interaction between the iminonitroxide and Cu(II) moieties was estimated using eq 3[21] to be a large, positive value (J/k_B = +510 K).

These iminonitroxide-Cu(II) moieties form a Cu_2O_2 cluster (formulated $[Cu(hfac)\cdot\mathbf{3}]_2$-A in Figure 7). Since the magnetic interaction within the iminonitroxide-Cu(II) moieties is strongly ferromagnetic as estimated (J/k_B = +510 K in Table 2), two spin configurations for the Cu_2O_2 cluster are possible; ($[Cu(hfac)\cdot\mathbf{3}]_2$-B and C in Figure 7). From the energy difference (ΔE = −29.3 K in Table 2) between the high-spin (**B**, $E_{Stotal=2}$ = −6654.23070691 au, $\langle S^2 \rangle$ = 6.0212) and low-spin (**C**, $E_{Stotal=0}$ = −6654.23079997 au, $\langle S^2 \rangle$ = 2.0173) states, the low-spin state **C** was shown to be slightly stable, showing an antiferromagnetic interaction of J/k_B = −7.33 K.[21] This calculated value is compatible with the observed maximum in the χ_p-T plot (Figure 5, inset).

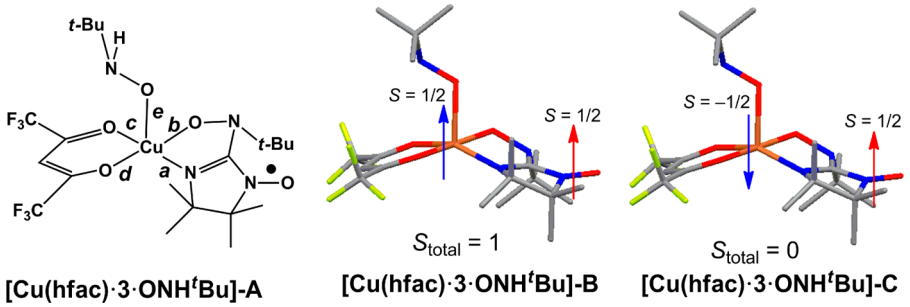

Figure 6. Model structure (**A**: bond length: *a*: 1.960(2) Å, *b*: 1.921(2) Å, *c*: 1.997(2) Å, *d*: 1.951(2) Å, *e*: 2.199(2) Å) and possible spin configurations of the partial structure around iminonitroxide-Cu(II) taken from X-ray structure, **B**: high-spin configuration (S_{total} = 1) and **C**: low-spin configuration (S_{total} = 0).

dx.doi.org/10.1021/ic4020898 | Inorg. Chem. 2014, 53, 802−809

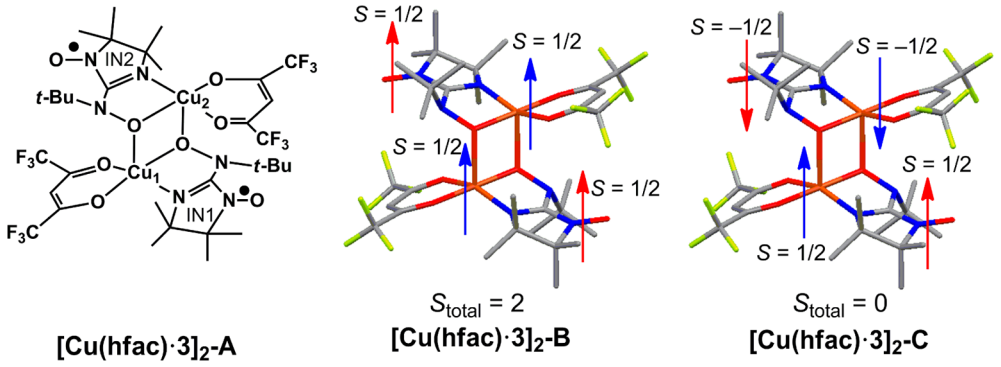

Figure 7. Chemical model structure (**A**) and possible spin configurations of the partial structure around Cu_2O_2 taken from the X-ray structure, **B**: high-spin configuration (S_{total} = 2) and **C**: low-spin configuration (S_{total} = 0).

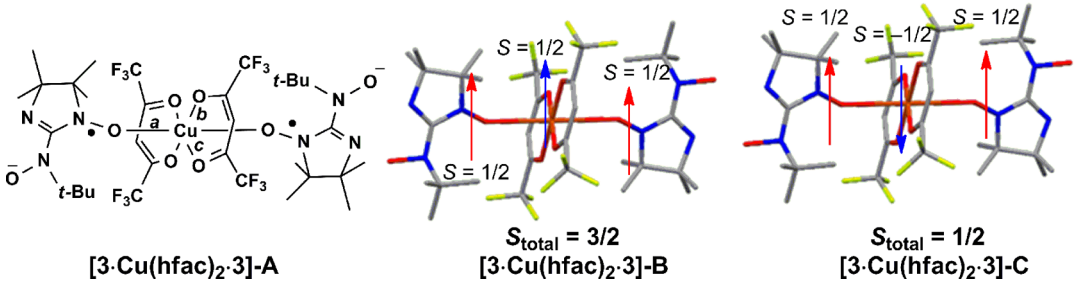

Figure 8. Model structure (**A**: *a*: 2.703(2) Å *b*: 1.924(2) Å, *c*: 1.913(2) Å) and spin structures taken from the X-ray structure, **B**: high-spin structure (S_{total} = 3/2) and **C**: low-spin structure (S_{total} = 1/2).

The iminonitroxides attached to the Cu_2O_2 cluster are axially bound to the Cu(II) atom in $Cu(hfac)_2$ (formulated by [**3**·$Cu(hfac)_2$·**3**]-A, B, C in Figure 8). Such an axial coordination on the Cu(II) atom has been established to show a ferromagnetic interaction (Gatteschi, Rey, and co-workers).[23] In accordance with their findings, the magnetic interaction was calculated to be J/k_B = +57.6 K (Table 2) from the energy difference (ΔE = 114 K) between the high-spin (**B**, $E_{Stotal=3/2}$ = −5013.82350479 au, $\langle S^2\rangle$ = 4.0151) and low-spin (**C**, $E_{Stotal=1/2}$ = −5013.82314218 au, $\langle S^2\rangle$ = 2.0293) states.

These theoretically analyzed magnetic interactions correlate approximately to the observed temperature dependence of χ_pT. To demonstrate that the above theoretical treatments provide reasonable values of the magnetic interactions in the linear chain complex $[Cu_2(hfac)_2\cdot\mathbf{3}_2\cdot Cu(hfac)_2]_n$, we considered two extreme cases of the thermal energy k_BT compared with the exchange interactions within the chain. In the high-temperature region (200−300 K in Figure 5 for the χ_pT−T plot and in Supporting Information, Figure S1 for the χ_pT−log T plot), we assumed a ferromagnetic model for a spin-1/2 pentamer (Scheme 3 top, corresponding to the structure in the box bracket in Scheme 2, eq 4)

$$H = -2J_1[\mathbf{S}_1(\mathrm{Cu})\cdot\mathbf{S}_2(\mathbf{3}) + \mathbf{S}_4(\mathbf{3})\cdot\mathbf{S}_5(\mathrm{Cu})] - 2J_2[\mathbf{S}_2(\mathbf{3})\cdot\mathbf{S}_3(\mathrm{Cu}) + \mathbf{S}_3(\mathrm{Cu})\cdot\mathbf{S}_4(\mathbf{3})] \quad (4)$$

where $\mathbf{S}_1$(Cu) and $\mathbf{S}_5$(Cu) are the S = 1/2 spins of Cu(II) in the Cu_2O_2 units, and $\mathbf{S}_2(\mathbf{3})$ and $\mathbf{S}_4(\mathbf{3})$ represent those of the radical anion **3**. The $\mathbf{S}_3$(Cu) spin is assigned to $Cu(hfac)_2$ at the inversion center. The numerical diagonalization of the spin Hamiltonian (eq 4) afforded energy eigenvalues, from which the temperature dependence of the magnetic susceptibility was calculated using eq 2. The simulation using J_1/k_B = +510 K, J_2/k_B = +58 K, with θ fixed to zero in eq 2, is shown by the dashed line in Figure 5. The simulation line approximately reproduces the χ_pT values between 200 and 300 K, although considerable deviation is observed below 200 K, where antiferromagnetic exchange interactions between the pentamers should be operative through the Cu_2O_2 units.

In the low-temperature region (<10 K), we applied an antiferromagnetic regular chain model (Scheme 3 below, eq 5):

$$H = -2J\sum_i \mathbf{S}_i\cdot\mathbf{S}_{i+1} \quad (5)$$

composed of S_i = 5/2 spins for the pentamers. The temperature dependence of magnetic susceptibility was analyzed using the Fisher chain model based on the classical spin approximation using eqs 6 and 7:[24]

$$\chi_p = [2Ng^2\mu_B^2/(3k_BT)][(1+u)/(1-u)] \quad (6)$$

$$u = \coth[2JS(S+1)/(k_BT)] - k_BT/[2JS(S+1)] \quad (7)$$

Scheme 3. Spin-Models for Magnetic Interactions in $[Cu_2(hfac)_2\cdot\mathbf{3}_2\cdot Cu(hfac)_2]_n$ at High and Low Temperatures

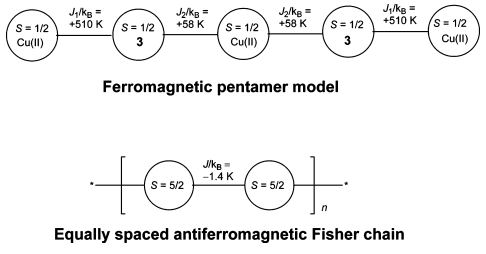

dx.doi.org/10.1021/ic4020898 | Inorg. Chem. 2014, 53, 802−809

The antiferromagnetic interaction J/k_B was optimized to fit the experimental data below 10 K (Figure 5 (Supporting Information, Figure S1) solid line), and it was estimated to be $J/k_B = -1.4$ K throughout the Cu_2O_2 framework ($\angle$Cu−O−Cu = 97.4°). The simulated J value is smaller than the calculated antiferromagnetic exchange interaction at −7.33 K (Table 2). Interestingly, the estimated value by simulation ($J/k_B = -1.4$ K) is compatible with the J/k_B−$\angle$Cu−O−Cu relationship observed by Hatfield and co-workers in the simpler hydroxo-bridged Cu dimer.[19]

CONCLUSION

We studied $Mn(hfac)_2$- and $Cu(hfac)_2$-complexation with a stable *N*-*t*-butyl-*N*-oxidanyl-2-amino-(nitronyl nitroxide) diradical (**1**). The formation of the complex was sensitive to the type of metal ion used. $[Mn(hfac)_2\cdot\mathbf{1}]$ was easily prepared. However, mixing of either **1** or **2** with $Cu(hfac)_2$ induced the transformation of the diradicals to radical anion **3**, producing the same complex $[Cu_2(hfac)_2\cdot\mathbf{3}_2\cdot Cu(hfac)_2]_n$ from both **1** and **2**. The molecular and packing structures of $[Mn(hfac)_2\cdot\mathbf{1}]$ and $[Cu_2(hfac)_2\cdot\mathbf{3}_2\cdot Cu(hfac)_2]_n$ were studied in detail. The magnetic properties of these complexes were investigated by measuring the temperature dependence of magnetic susceptibility. Their exchange interactions were determined with the aid of quantum calculations. $[Mn(hfac)_2\cdot\mathbf{1}]$ was characterized by a strong antiferromagnetic intramolecular magnetic interaction ($H = -2J\boldsymbol{S}_1\cdot\boldsymbol{S}_2$, $J/k_B = -217$ K) between diradical **1** ($S = 1$) and the Mn(II) atom ($S = 5/2$) with an intermolecular magnetic interaction ($\theta = -1.40$ K). $[Cu_2(hfac)_2\cdot\mathbf{3}_2\cdot Cu(hfac)_2]_n$ was characterized by a strongly ferromagnetic intramolecular interaction ($H = -2J\boldsymbol{S}_1\cdot\boldsymbol{S}_2$, $J/k_B = +510$ K) between the iminonitroxide moiety in **3** and the imino-coordinating Cu(hfac), a moderately large ferromagnetic intramolecular interaction ($H = -2J\boldsymbol{S}_1\cdot\boldsymbol{S}_2$, $J/k_B = -58$ K) between the iminonitroxide moieties in **3** and the iminonitroxide oxygen-coordinating $Cu(hfac)_2$, and a weak antiferromagnetic interaction ($H = -2J\boldsymbol{S}_1\cdot\boldsymbol{S}_2$, $J/k_B = -1.4$ K) between two Cu(hfac)·**3** moieties within the Cu_2O_2 framework.

ASSOCIATED CONTENT

Supporting Information

Crystallographic information files (cif) for $[Mn(hfac)_2\cdot\mathbf{1}]$ and $[Cu_2(hfac)_2\cdot\mathbf{3}_2\cdot Cu(hfac)_2]_n$, and the c_pT-log T plot for $[Cu_2(hfac)_2\cdot\mathbf{3}_2\cdot Cu(hfac)_2]_n$. This material is available free of charge via the Internet at http://pubs.acs.org.

AUTHOR INFORMATION

Corresponding Authors

*E-mail: okadak@sci.osaka-cu.ac.jp (K.O.).

*E-mail: Victor.Ovcharenko@tomo.nsc.ru (V.I.O.).

Present Address

[§]Sekisuiplastic Company, Japan.

Notes

The authors declare no competing financial interest.

ACKNOWLEDGMENTS

This study was supported by a Grant (# 22350066 (K.O.)) from JSPS, a financial support from the Asahi Glass Foundation, a Grant-in-Aid (25109537 (S.S.)) for Scientific Research on Innovative Areas "Stimuli-responsive Chemical Species for the Creation of Functional Molecules" from MEXT Japan; this work was also supported by the Russian Foundation for Basic Research (Grants 12-03-00067, 11-03-00027) and the Council for Grants at the President of the Russian Federation (Program for State Support of Young Scientists, Grant MK-5791.2013.3).

REFERENCES

(1) (a) *Molecular Magnetism*; Itoh, K., Kinoshita, M., Eds.; Kodansha & Gordon and Breach: Tokyo, Japan, 2000. (b) *Magnetism: Molecules to Materials II-V*; Miller, J. S., Drillon, M., Eds.; Wiley-VCH: Weinheim, Germany, 2001; (c) *π-Electron Magnetism from Molecules to Magnetic Materials*; Veciana, J., Ed.; Springer: Berlin, Germany, 2001.

(2) (a) Hicks, R. G. *Org. Biomol. Chem.* **2007**, *5*, 1321−1338. (b) *Stable Radicals: Fundamentals and Applied Aspects of Odd-Electron Compounds*; Hicks, R. G., Ed.; Wiley: Chichester, U.K., 2010.

(3) (a) Rajca, A.; Wongsriratanakul, J.; Rajca, S. *Science* **2001**, *294*, 1503−1505. (b) Masuda, Y.; Kuratsu, M.; Suzuki, S.; Kozaki, M.; Shiomi, D.; Sato, K.; Takui, T.; Hosokoshi, Y.; Lan, X.-Z.; Miyazaki, Y.; Inaba, A.; Okada, K. *J. Am. Chem. Soc.* **2009**, *131*, 4670−4673. (c) Kuratsu, M.; Suzuki, S.; Kozaki, M.; Shiomi, D.; Sato, K.; Takui, T.; Kanzawa, K.; Hosokoshi, Y.; Lan, X.-Z.; Miyazaki, Y.; Inaba, A.; Okada, K. *Chem.—Asian. J.* **2012**, *7*, 1604−1609. (d) Ovcharenko, V., Bagryanskaya, E. In *Spin-Crossover Materials: Properties and Applications*; Halcrow, M. A., Ed.; Wiley-Blackwell: Oxford, U.K., 2013; pp 239−280. (e) Ovcharenko, V. I.; Fokin, S. V.; Fursova, E. Yu.; Kuznetsova, O. V.; Tretyakov, E. V.; Romanenko, G. V.; Bogomyakov, A. S. *Inorg. Chem.* **2011**, *50*, 4307−4312.

(4) (a) Pal, S. K.; Itkis, M. E.; Tham, F. S.; Reed, R. W.; Oakley, R. T.; Haddon, R. C. *Science* **2005**, *309*, 281−284. (b) Iwasaki, A.; Hu, L.; Suizu, R.; Nomura, K.; Yoshikawa, H.; Awaga, K.; Noda, Y.; Kanai, K.; Ouchi, Y.; Seki, K.; Ito, H. *Angew. Chem., Int. Ed.* **2009**, *48*, 4022−4024.

(5) Sugawara, T.; Komatsu, H.; Suzuki, K. *Chem. Soc. Rev.* **2011**, *40*, 3105−3118.

(6) (a) Ovcharenko, V. I.; Fursova, E. Y.; Tolstikova, T. G.; Sorokina, K. N.; Letyagin, A. Y.; Savelov, A. A. *Dokl. Chem.* **2005**, *404*, 171−173. (b) Savelov, A. A.; Kokorin, D. A.; Fursova, E. Y.; Ovcharenko, V. I. *Dokl. Chem.* **2007**, *416*, 241−243.

(7) (a) Nishide, H.; Oyaizu, K. *Science* **2008**, *319*, 737−738. (b) Morita, Y.; Suzuki, S.; Sato, K.; Takui, T. *Nat. Chem.* **2011**, *3*, 197−204.

(8) (a) Coronado, E.; Epstein, A. J. *J. Mater. Chem.* **2009**, *19*, 1670−1671. (b) Coronado, E.; Day, P. *Chem. Rev.* **2004**, *104*, 5419−5548. (c) Enoki, T.; Miyazaki, A. *Chem. Rev.* **2004**, *104*, 5449−5477.

(9) (a) Sato, K.; Nakazawa, S.; Rahimi, R.; Ise, T.; Nishida, S.; Yoshino, T.; Mori, N.; Toyota, K.; Shiomi, D.; Yakiyama, Y.; Morita, Y.; Kitagawa, M.; Nakasuji, K.; Nakahara, M.; Hara, H.; Carl, P.; Höfer, P.; Takui, T. *J. Mater. Chem.* **2009**, *19*, 3739−3754. (b) Nakazawa, S.; Nishida, S.; Ise, T.; Yoshino, T.; Mori, N.; Rahimi, R. D.; Sato, K.; Morita, Y.; Toyota, K.; Shiomi, D.; Kitagawa, M.; Hara, H.; Carl, P.; Höfer, P.; Takui, T. *Angew. Chem., Int. Ed.* **2012**, *51*, 9860−9864. (c) Ayabe, K.; Sato, K.; Nakazawa, S.; Nishida, S.; Sugisaki, K.; Ise, T.; Morita, Y.; Toyota, K.; Shiomi, D.; Kitagawa, M.; Suzuki, S.; Okada, K.; Takui, T. *Mol. Phys.* **2013**, *111*, in press.

(10) (a) Borden, W. T. In *Diradicals*; Borden, W. T., Ed.; John Wiley & Sons: New York, 1982; pp 1−72. (b) Wenthold, P. G.; Hu, J.; Squires, R. R.; Lineberger, W. C. *J. Am. Chem. Soc.* **1996**, *118*, 475−476.

(11) Dowd, P.; Chow, M. *J. Am. Chem. Soc.* **1977**, *99*, 6438−6440.

(12) (a) Mukai, K.; Ishizu, K.; Deguchi, Y. *J. Phys. Soc. Jpn.* **1969**, *27*, 783. (b) Iwamura, H.; Inoue, K. In *Magnetism: Molecules to Materials II*; Miller, J. S., Drillon, M., Eds.; Wiley-VCH; New York, 2001; pp 61−108. (c) Shultz, D. A. In *Magnetic Properties of Organic Materials*; Lahti, P. M., Ed.; Marcell Dekker: New York, 1999; pp 103−146. (d) Hiraoka, S.; Okamoto, T.; Kozaki, M.; Shiomi, D.; Sato, K.; Takui, T.; Okada, K. *J. Am. Chem. Soc.* **2004**, *126*, 58−59. (e) Rajca, A.; Shiraishi, K.; Pink, M.; Rajca, S. *J. Am. Chem. Soc.* **2007**, *129*, 7232−7233. (f) Rajca, A.; Shiraishi, K.; Rajca, S. *Chem. Commun.* **2009**,

4372−4374. (g) Suzuki, S.; Nagata, A.; Kuratsu, M.; Kozaki, M.; Tanaka, R.; Shiomi, D.; Sugisaki, K.; Toyota, K.; Sato, K.; Takui, T.; Okada, K. *Angew. Chem., Int. Ed.* **2012**, *51*, 3193−3197.
(13) (a) Suzuki, S.; Furui, T.; Kuratsu, M.; Kozaki, M.; Shiomi, D.; Sato, K.; Takui, T.; Okada, K. *J. Am. Chem. Soc.* **2010**, *132*, 15908−15910. (b) Tretyakov, E. V.; Tolstikov, S. E.; Romanenko, G. V.; Bogomyakov, A. S.; Stass, D. V.; Maryasov, A. G.; Gritsan, N. P.; Ovcharenko, V. I. *Russ. Chem. Bull.* **2011**, *60*, 2608−2612.
(14) Only a few examples of diradical−coordinated metal complexes have been reported: (a) Caneschi, A.; Dei, A.; Lee, H.; Shultz, D. A.; Sorace, L. *Inorg. Chem.* **2001**, *40*, 408−411. (b) Bodnar, S. H.; Caneschi, A.; Dei, A.; Shultz, D. A.; Sorace, L. *Chem. Commun.* **2001**, 2150−2151. (c) Fatila, E. M.; Clérac, R.; Rouzières, M.; Soldatov, D. V.; Jennings, M.; Preuss, K. E. *J. Am. Chem. Soc.* **2013**, *135*, 13298−13301.
(15) Nakatsuji, S.; Takai, A.; Ojima, T.; Anzai, H. *J. Chem. Res., Synop.* **1999**, 620−621.
(16) Osiecki, J. H.; Ullman, E. F. *J. Am. Chem. Soc.* **1968**, *90*, 1078−1079.
(17) Tretyakov, E.; Tolstikov, S.; Mareev, A.; Medvedeva, A.; Romanenko, G.; Stass, D.; Bogomyakov, A.; Ovcharenko., V. *Eur. J. Org. Chem.* **2009**, 2548−2561.
(18) Typical examples: (a) *Magneto-Structural Correlations in Exchange Coupled Systems*; Willett, R. D., Gatteschi, D., Kahn, O., Eds.; Reidel: Dordrecht, The Netherlands, 1985. (b) Cairns, C. J.; Busch, D. *Coord. Chem. Rev.* **1986**, *69*, 1−55. (c) Chiari, B.; Piovesana, O.; Tarantelli, T.; Zanazzi, P. F. *Inorg. Chem.* **1988**, *27*, 4149−4153.
(19) Crawford, V. H.; Richardson, H. W.; Wasson, J. R.; Hodgson, D. J.; Hatfield, W. E. *Inorg. Chem.* **1976**, *15*, 2107−2110.
(20) Frisch, M. J.; Trucks, G. W.; Schlegel, H. B.; Scuseria, G. E.; Robb, M. A.; Cheeseman, J. R.; Scalmani, G.; Barone, V.; Mennucci, B.; Petersson, G. A.; Nakatsuji, H.; Caricato, M.; Li, X.; Hratchian, H. P.; Izmaylov, A. F.; Bloino, J.; Zheng, G.; Sonnenberg, J. L.; Hada, M.; Ehara, M.; Toyota, K.; Fukuda, R.; Hasegawa, J.; Ishida, M.; Nakajima, T.; Honda, Y.; Kitao, O.; Nakai, H.; Vreven, T.; Montgomery, Jr., J. A.; Peralta, J. E.; Ogliaro, F.; Bearpark, M.; Heyd, J. J.; Brothers, E.; Kudin, K. N.; Staroverov, V. N.; Kobayashi, R.; Normand, J.; Raghavachari, K.; Rendell, A.; Burant, J. C.; Iyengar, S. S.; Tomasi, J.; Cossi, M.; Rega, N.; Millam, J. M.; Klene, M.; Knox, J. E.; Cross, J. B.; Bakken, V.; Adamo, C.; Jaramillo, J.; Gomperts, R.; Stratmann, R. E.; Yazyev, O.; Austin, A. J.; Cammi, R.; Pomelli, C.; Ochterski, J. W.; Martin, R. L.; Morokuma, K.; Zakrzewski, V. G.; Voth, G. A.; Salvador, P.; Dannenberg, J. J.; Dapprich, S.; Daniels, A. D.; Farkas, Ö.; Foresman, J. B.; Ortiz, J. V.; Cioslowski, J.; Fox, D. J. *Gaussian 09*, Revision A.02; Gaussian, Inc.: Wallingford, CT, 2009.
(21) (a) Yamaguchi, K.; Kawakami, T.; Takano, Y.; Kitagawa, Y.; Yamashita, Y.; Fujita, H. *Int. J. Quantum Chem.* **2002**, *90*, 370−385. (b) Ruiz, E.; Cano, J.; Alvarez, S.; Alemany, P. *J. Comput. Chem.* **1999**, *20*, 1391−1400.
(22) Luneau, D.; Rey, P.; Laugier, J.; Fries, P.; Caneschi, A.; Gatteschi, D.; Sessoli, R. *J. Am. Chem. Soc.* **1991**, *113*, 1245−1251.
(23) (a) Caneschi, A.; Gatteschi, D.; Laugier, J.; Rey, P. *J. Am. Chem. Soc.* **1987**, *109*, 2191−2192. (b) Cabello, C. I.; Caneschi, A.; Carlin, R. L.; Gatteschi, D.; Rey, P.; Sessoli, R. *Inorg. Chem.* **1990**, *29*, 2582−2587.
(24) Fisher, M. E. *Am. J. Phys.* **1964**, *32*, 343−346.